

frustration-induced phase transitions in the spin- S orthogonal-dimer chain

Akihisa Koga and Norio Kawakami

Department of Applied Physics, Osaka University, Suita, Osaka 565-0871, Japan

(Dated: November 20, 2018)

We investigate quantum phase transitions in the frustrated orthogonal-dimer chain with an arbitrary spin $S \geq 1/2$. When the ratio of the competing exchange couplings is varied, first-order phase transitions occur $2S$ times among distinct spin-gap phases. The introduction of single-ion anisotropy further enriches the phase diagram. The phase transitions described by the present model possess most of the essential properties inherent in frustrated quantum spin systems.

Geometrical frustration in strongly correlated electron systems has attracted much current interest. A remarkable example of materials is the two-dimensional spin-gap compound $\text{SrCu}_2(\text{BO}_3)_2$, [1] in which the characteristic orthogonal-dimer structure of the Cu^{2+} ions stabilizes the spin-singlet ground state. [2, 3, 4] Remarkably, strong frustration induces an anomalous first-order phase transition in addition to the plateau-formation in the magnetization process. [5] More recently, another orthogonal-dimer compound $\text{Nd}_2\text{BaZnO}_5$ [6] was synthesized, where higher-spin and orbital moments ($J = 9/2$) show the antiferromagnetic order at the critical temperature $T_N = 2.4\text{K}$, making such higher-spin systems more interesting.

One of the most prototypical phenomena inherent in the frustrated systems is the *first-order* transition, which is triggered by the competition of various phases due to strong frustration. Although the systematic treatment of first-order transitions is not easy, it is highly desirable to clarify how such first-order transitions are induced by frustration in order to understand the essential properties common to such frustrated quantum spin systems.

In this paper, we investigate a remarkable one-dimensional (1D) spin- S orthogonal-dimer model, which possesses most of the essential properties of first-order phase transitions in this class of frustrated spin systems. [7, 8, 9, 10] By exploiting the non-linear sigma model (NL σ M) approach as well as the exact diagonalization and the series expansion, we find the $(2S + 1)$ distinct spin-gap phases in the spin- S chain, which are separated by first-order quantum phase transitions. The effect of single-ion anisotropy is also addressed. We demonstrate that a higher-spin generalization of the model results in the remarkably rich phase diagram, which realizes the idea of valence-bond-solid (VBS) [11] in a *sequence of first-order phase transitions*.

Let us consider the 1D quantum spin system with the orthogonal-dimer structure [8, 9, 10] shown schematically in Fig. 1. The corresponding Hamiltonian reads

$$H = J \sum_j (\mathbf{S}_{2,j} \cdot \mathbf{S}_{4,j} + \mathbf{S}_{3,j} \cdot \mathbf{S}_{1,j+1}) + J' \sum_j (\mathbf{S}_{2,j} + \mathbf{S}_{4,j}) \cdot (\mathbf{S}_{1,j} + \mathbf{S}_{3,j}), \quad (1)$$

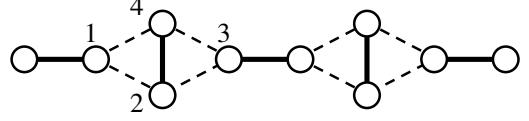


FIG. 1: Orthogonal-dimer spin chain: the dimer bonds shown by solid lines have the characteristic orthogonal structure.

where $\mathbf{S}_{i,j}$ is the i -th spin operator in the j -th plaquette and $J(J')$ is the antiferromagnetic exchange coupling. The $S = 1/2$ model was so far studied well. [9, 10] Below, we focus on a higher-spin generalization of the system.

We first exploit the NL σ M technique to clarify the topological nature of the system. [12, 13, 14, 15, 16] Note that the Hamiltonian has the remarkable relation $[H, \mathbf{S}_{2,j} + \mathbf{S}_{4,j}] = 0$. Therefore, by introducing the composite spin T_j defined as $\mathbf{T}_j = \mathbf{S}_{2,j} + \mathbf{S}_{4,j}$, we obtain the effective mixed-spin Hamiltonian as, $H = \sum [J' \mathbf{S}_{1j} \cdot \mathbf{T}_j + J' \mathbf{T}_j \cdot \mathbf{S}_{3j} + J \mathbf{S}_{3j} \cdot \mathbf{S}_{1j+1}] + \frac{J}{2} \sum T_j (T_j + 1) - \frac{1}{4} J S(S+1)N$, where N is the total number of sites. Then, the Hilbert space of the Hamiltonian (1) can be classified into each sub-space specified by $[S; \{T_j\}]$. The singlet ground state as well as relevant low-energy excitations are in the space with uniform $T_j (= T)$. In particular, for a given $T \neq 0$ we can describe low-energy properties by the NL σ M ($T = 0$ gives a trivial system with decoupled dimers). Introducing three kinds of the fluctuation fields, [14, 15, 16] we obtain the Euclidean Lagrangian \mathcal{L} with the effective field ϕ as,

$$\mathcal{L} = \frac{1}{2g} \left(v_s \phi'^2 + \frac{1}{v_s} \dot{\phi}^2 \right) - \frac{i\theta}{4\pi} \phi \cdot (\phi' \times \dot{\phi}), \quad (2)$$

where $\theta = 2\pi T$, $g = 2AB/T$, $v_s = 6J'StB/A$ with $A = (2t + j_0)^{1/2}$, $B = [4j_0t^2 + 2(1 - 2j_0)t + j_0]^{-1/2}$, $j_0 = J'/J$ and $t = S/T$. Note that the topological angle θ is zero (mod 2π) for any choice of T , and the system is always gapped. Therefore, in case the phase transition between the distinct sub-spaces $[S; \{T_j\}]$ occurs, it should be accompanied by the discontinuity in the parameters g and v_s . This suggests that the possible quantum phase transition should be of *first-order*.

To clarify this point, we numerically diagonalize the Hamiltonian (1) for a small cluster with periodic boundary conditions. The ground state energy is shown in Fig.

2. It is found that the cusps appear $2S$ times in the

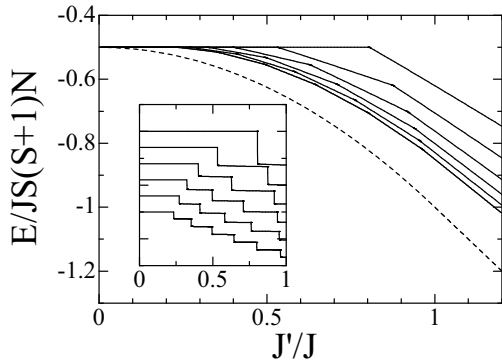


FIG. 2: Ground-state energy as a function of J'/J obtained by the exact diagonalization for 8 sites. From up to down $S = 1/2, 1, 3/2, 2, 5/2, 3$. The broken line is the energy for the classical limit $S \rightarrow \infty$. The inset shows the derivative of the ground state energy, in which the origin for each curve is shifted for convenience.

energy diagram for the spin- S case, implying that the *first-order* quantum phase transitions indeed occur $2S$ times. Also shown is the energy in the classical limit $S \rightarrow \infty$, which is given as $E/JS^2N = -\frac{1}{2}[1 + (J'/J)^2]$, and $-J'/J$ for the helical phase ($0 < J'/J < 1$) and the antiferromagnetically ordered phase ($1 < J'/J$). As S increases, the profile of the energy diagram gradually approaches the classical one, although the $2S$ transitions should exist for any finite S . By examining several systems with different cluster size, we determine the phase diagram rather precisely, as shown in Fig. 3. In this

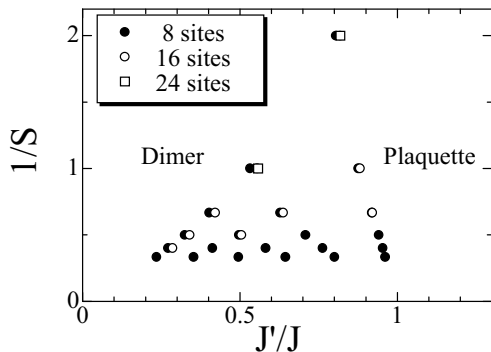


FIG. 3: Ground-state phase diagram for the orthogonal-dimer spin chain with generic spin S . The closed circles, open circles and open squares indicate the phase boundaries determined by the spin chain ($N = 8, 16, 24$) with periodic boundary conditions.

way, the present model is the remarkable spin- S microscopic model, which clearly determines a sequence of the phase transitions triggered by frustration. Moreover, the *first-order* transitions found here are contrasted to the *second-order* ones known for the ordinary spin- S Heisenberg chain with bond alternation.[13]

We now clarify the nature of each spin-gap phase by taking the $S = 1$ model as an example, which contains three distinct spin-gap phases. For this purpose, the VBS description [11] of the ground state is useful, where the topological nature is specified by a combination of singlet bonds between the decomposed $S = 1/2$ spins, as shown in Fig. 4. Recall that in the small (large) J'/J region,

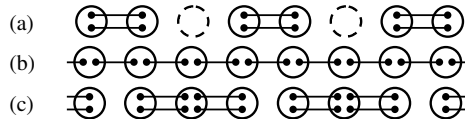


FIG. 4: VBS picture of the phases for the $S = 1$ model.

the composite spin $T = 0(2)$ on each diagonal bond is realized. Hence the dimer (plaquette) phase characterized by Fig. 4 (a) [(c)] is stabilized there. On the other hand, in the intermediate phase, strong frustration induces the spin $T = 1$ on each diagonal bond, resulting in the singlet phase characterized by Fig. 4(b). This may be regarded as the *frustration-induced Haldane phase*.

To confirm the above predictions based on the VBS analysis, we perform the numerical diagonalization of small clusters in the corresponding sub-spaces. In Fig.

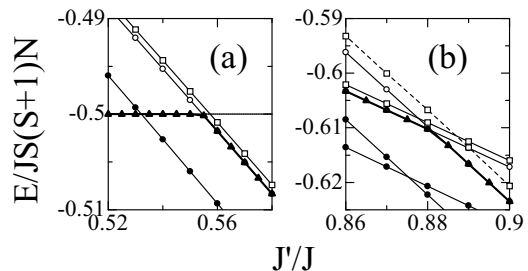


FIG. 5: The energy for the $S = 1$ orthogonal-dimer spin chain in the restricted sub-space.

5 (a), the flat line is the energy for the exact dimer state. The energy for the Haldane phase ($N = 8, 16$ and 24) obtained by the exact diagonalization in the sub-space $\{|T_j = 1\rangle\}$ is shown as the solid line with closed circles, open circles and open squares, respectively. We also show the ground state energy of the original orthogonal-dimer spin chain ($N = 16$) as the bold line with closed triangles. As seen clearly, the increase of J'/J triggers the first-order quantum phase transition from the dimer phase ($T_j = 0$) to the Haldane phase ($T_j = 1$) at the critical value $(J'/J)_c \sim 0.56$. Shown in Fig. 5 (b) is the energy around the other first-order critical point between the Haldane phase ($T_j = 1$) and the plaquette phase ($T_j = 2$). In the plaquette phase, we have used the series expansion [17] by choosing an isolated plaquette as the unperturbed system and regarding the interaction between plaquettes as a perturbation. The ground state energy calculated up to the ninth order is shown as the

broken line in Fig. 5, from which we find the critical point $(J'/J)_c \sim 0.88$ between the Haldane and the plaquette phases. It is thus concluded that the first-order quantum phase transitions occur among three singlet phases specified by the distinct sub-spaces $[S; \{T_j\}] (T_j = 0, 1, 2)$, as predicted by the NL σ M approach.

Keeping this in mind, we now consider excitations in the $S = 1$ orthogonal-dimer spin chain. In the dimer

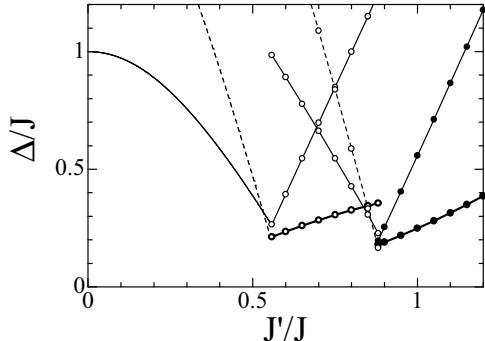


FIG. 6: Various excitations in the $S = 1$ orthogonal-dimer spin chain. The bold lines indicate a dispersive magnetic excitation, while the solid (broken) lines dispersionless magnetic (non-magnetic) excitations.

phase ($J'/J < 0.56$), the ground state is given by the product of isolated dimers $[\{T_j = 0\}]$, which allows us to estimate the excitation gap exactly from the finite-size calculation. The lowest magnetic excitation is described by a defect in the uniform spin alignment, *i.e.*, it is given by the lowest triplet state in the space of $[1, 0, 0, 0, \dots]$. It is also found that in the vicinity of the critical point ($J'/J \sim 0.56$), a non-magnetic excitation belonging to the space $[1, 1, 0, 0, 0, \dots]$ can be the lowest one, as shown by the broken line. In the Haldane phase ($0.56 < J'/J < 0.88$), we estimate several kinds of spin gaps by extrapolating the results for $N = 16, 24$ in the formula $\Delta(N) = \Delta(\infty) + aN^{-2}$. The Haldane gap expected naively is the lowest away from the critical points, shown as the bold line in Fig. 6. There are other dispersionless excitations, which can be described by a defect in the spin alignment such as $[0, 1, 1, 1, \dots]$, $[2, 1, 1, 1, \dots]$. These excitations are bound into another non-magnetic state, which is the lowest excitation in the Haldane phase close to the plaquette phase ($J'/J \sim 0.88$). In the plaquette phase ($0.88 < J'/J$), the series expansion is more efficient to obtain the dispersive and the dispersionless excitations. The results computed up to the seventh and the ninth order are shown as the closed circles in Fig. 6. In this way, several different excitations become almost degenerate around the first-order phase transition points, reflecting strong frustration.

Finally we discuss the effect of single-ion anisotropy with the Hamiltonian $H_D = D \sum (S_{i,j}^z)^2$. The composite spin T_j is not a good quantum number in the presence of the D -term. The frustration-induced interme-

diated phases, however, are stable against the introduction of small anisotropy. In fact, the cusps still exist in the energy diagram for the spin $S = 1$ chain ($N = 16$), from which we determine the phase boundaries shown as the open circles in Fig. 7. The Haldane phase grad-

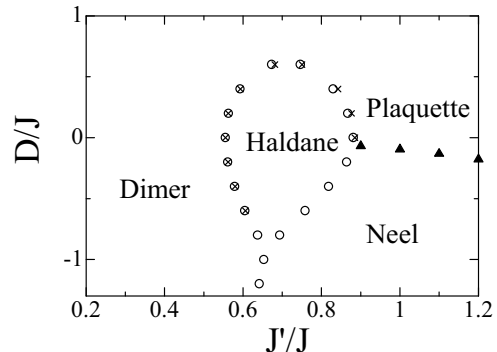


FIG. 7: Phase diagram for the anisotropic $S = 1$ chain with the orthogonal-dimer structure.

ually shrinks with the increase of $D (> 0)$, and finally disappears. We note that around $D \gtrsim 0.8$ the dimer and the plaquette phases indeed merge into the single phase. In order to clearly distinguish the Haldane phase and the dimer (or plaquette) phase, we make use of the symmetry of the space inversion P and the spin reversal τ . Under twisted boundary conditions[18] ($S_{1,N/4+1}^x = -S_{1,1}^x, S_{1,N/4+1}^y = -S_{1,1}^y, S_{1,N/4+1}^z = S_{1,1}^z$), the dimer or plaquette state has the eigenvalues $P = \tau = 1$, while the Haldane state $P = \tau = -1$. Therefore, we can distinguish these phases by diagonalizing the Hamiltonian with twisted boundary in the restricted space specified by $P = \tau = \pm 1$. The results for $D = 0.4$ are shown in Fig. 8. It is found that the two lowest energy levels intersect

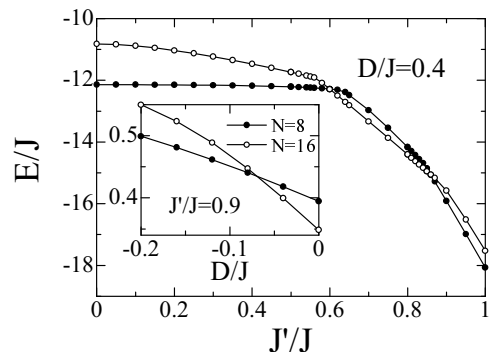


FIG. 8: Two lowest energies with twisted boundary conditions for $N = 16$ and $D = 0.4$. The energy of the Haldane state ($P = \tau = -1$) and the dimer or the plaquette state ($P = \tau = 1$) are shown by the open and closed circles. The inset shows the Binder parameter U_{Neel} for $J'/J = 0.9$. The closed and open circles ($N = 8$ and 16) are calculated with periodic boundary conditions.

each other twice when the ratio of the exchange coupling

J'/J is varied. This implies that the quantum phase transitions between the phases with distinct symmetry ($P = \tau = \pm 1$) occur twice, being consistent with the above predictions based on the VBS analysis. By scaling the critical values as $(J'/J)_c(N) = (J'/J)_c(\infty) + aN^{-2}$, we estimate the phase boundaries shown as the crosses in Fig. 7, which agree well with those determined from the original plaquette chain ($N = 16$) shown as open circles. In contrast, when D is negative, the antiferromagnetic correlation is enhanced, and the systems is driven to the Neel ordered phase. To characterize this transition, we check the behavior of the Binder parameter, $U_{Neel} = 1 - \frac{\langle O^4 \rangle}{3\langle O^2 \rangle^2}$, where O is the order parameter defined as $O = \sum (-1)^{i+j} S_{i,j}^z$. In the inset of Fig. 8, the Binder parameters for $N = 8$ and 16 are shown as a function of D with $J'/J = 0.9$. Since the Binder parameter stays invariant with the change of N at the transition point, we can determine the critical value $(D/J)_c \sim -0.07$. Consequently, we end up with the phase diagram for the spin $S = 1$ chain with anisotropy as shown in Fig. 7.

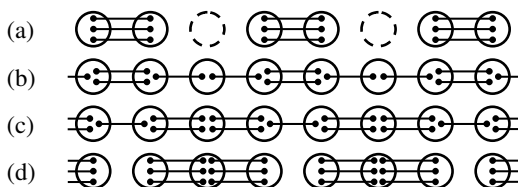


FIG. 9: VBS picture of the phases for the $S = 3/2$ model.

In summary, we have studied the spin- S quantum spin chain with the orthogonal-dimer structure. The obtained phase diagram has a rich structure with various type of spin-gap phases which are separated by first-order phase transitions inherent in fully frustrated systems. Although we have given detailed accounts for the $S = 1$ case, it is straightforward to generalize the discussions to an arbitrary-spin case. For example, four distinct spin-gap phases for $S = 3/2$ in Fig. 3 are completely classified by the VBS states shown in Fig. 9. Finally we emphasize that the first-order phase transitions in the present model are triggered by strong frustration, which may capture most of essential properties common to this class of fully frustrated systems. In particular, we think that

frustration-induced spin-gap phases obtained here may play a key role to clarify the phase diagram of the 2D spin- S orthogonal-dimer model.

This work was partly supported by a Grant-in-Aid from the Ministry of Education, Science, Sports and Culture of Japan. A part of computations was done at the Supercomputer Center at the Institute for Solid State Physics, University of Tokyo and Yukawa Institute Computer Facility.

-
- [1] H. Kageyama, *et al.*, Phys. Rev. Lett. **82** 3168 (1999).
 - [2] B. S. Shastry and B. Sutherland, Physica **108B** 1069 (1981).
 - [3] S. Miyahara and K. Ueda, Phys. Rev. Lett. **82** 3701 (1999).
 - [4] A. Koga and N. Kawakami, Phys. Rev. Lett. **84**, 4461 (2000); C. Knetter, *et al.*, Phys. Rev. Lett. **85**, 3958 (2000); T. Momoi and K. Totsuka, Phys. Rev. B **61** 3231 (2000); Y. Fukumoto, J. Phys. Soc. Jpn. **69**, 2755 (2000); G. Misguich, *et al.*, Phys. Rev. Lett. **87** 097203 (2001); C. H. Chung, *et al.*, Phys. Rev. B **64** 134407 (2001); W. Zheng, *et al.*, Phys. Rev. B **65**, 014408 (2002).
 - [5] K. Onizuka, *et al.*, J. Phys. Soc. Jan. **69**, 1016 (2000).
 - [6] H. Kageyama, *et al.*, preprint.
 - [7] Y. Takushima, A. Koga and N. Kawakami, J. Phys. Soc. Jpn. **70** (2001) 1369.
 - [8] N. Kato and M. Imada, J. Phys. Soc. Jpn. **64**, (1995) 4105.
 - [9] N. B. Ivanov and J. Richter, Phys. Lett. **232A**, 308 (1997); J. Phys. Condence Matt. **10**, 3635 (1998); Phys. Rev. B **65**, 054420 (2002).
 - [10] A. Koga, K. Okunishi and N. Kawakami, Phys. Rev. B **62**, 5558 (2000).
 - [11] I. Affleck, *et al.*, Phys. Rev. Lett. **59** 799 (1987); Commun. Math. Phys. **115** 477 (1988).
 - [12] F. D. M. Haldane, Phys. Lett. **93A** 464 (1983); Phys. Rev. Lett. **50** 1153 (1983).
 - [13] I. Affleck and F. D. M. Haldane, Phys. Rev. B **36** 5291 (1987).
 - [14] T. Fukui and N. Kawakami, Phys. Rev. B **55** (1997) R14709; Phys. Rev. B **56** (1997) 8799.
 - [15] A. Koga, S. Kumada, N. Kawakami and T. Fukui, J. Phys. Soc. Jpn. **67** (1998) 622.
 - [16] K. Takano, Phys. Rev. Lett. **82**, (1999) 5124.
 - [17] M. P. Gelfand and R. R. P. Singh, Adv. Phys. **49**, 93 (2000).
 - [18] A. Kitazawa and K. Nomura, J. Phys. Soc. Jpn. **66**, 3944 (1997).